The sulphur oxygenase reductase from *Acidianus ambivalens* is a multimeric protein containing a low-potential mononuclear non-haem iron centre

Tim URICH*, Tiago M. BANDEIRAS†, Sónia S. LEAL†, Reinhard RACHEL‡, Till ALBRECHT*, Peter ZIMMERMANN*, Corinna SCHOLZ*, Miguel TEIXEIRA†, Cláudio M. GOMES†§ and Arnulf KLETZIN*[1]

*Institute of Microbiology and Genetics, Darmstadt University of Technology, Schnittspahnstrasse 10, 64287 Darmstadt, Germany, †Instituto de Tecnologia Química e Biológica, Universidade Nova de Lisboa, Rua da Quinta Grande 6, Apt 127, 2780-156, Oeiras, Portugal, ‡Department of Microbiology and Archaeenzentrum, Universitätsstrasse 31, 93053 Regensburg, Germany, and §Departamento de Química, Faculdade de Ciências e Tecnologia, Universidade Nova de Lisboa, 2825-114 Caparica, Portugal

The SOR (sulphur oxygenase reductase) is the initial enzyme in the sulphur-oxidation pathway of *Acidianus ambivalens*. Expression of the *sor* gene in *Escherichia coli* resulted in active, soluble SOR and in inclusion bodies from which active SOR could be refolded as long as ferric ions were present in the refolding solution. Wild-type, recombinant and refolded SOR possessed indistinguishable properties. Conformational stability studies showed that the apparent unfolding free energy in water is approx. 5 kcal · mol^{-1} (1 kcal = 4.184 kJ), at pH 7. The analysis of the quaternary structures showed a ball-shaped assembly with a central hollow core probably consisting of 24 subunits in a 432 symmetry. The subunits form homodimers as the building blocks of the holoenzyme. Iron was found in the wild-type enzyme at a stoichiometry of one iron atom/subunit. EPR spectroscopy of the colourless SOR resulted in a single isotropic signal at $g = 4.3$, characteristic of high-spin ferric iron. The signal disappeared upon reduction with dithionite or incubation with sulphur at elevated temperature. Thus both EPR and chemical analysis indicate the presence of a mononuclear iron centre, which has a reduction potential of -268 mV at pH 6.5. Protein database inspection identified four SOR protein homologues, but no other significant similarities. The spectroscopic data and the sequence comparison led to the proposal that the *Acidianus ambivalens* SOR typifies a new type of non-haem iron enzyme containing a mononuclear iron centre co-ordinated by carboxylate and/or histidine ligands.

Key words: electron paramagnetic resonance (EPR), hyperthermophilic archaea, quaternary structure, reversible denaturation, sulphur oxidation.

INTRODUCTION

Elemental sulphur and reduced inorganic sulphur compounds are metabolized by a large number of micro-organisms belonging to the domains of the Bacteria and the Archaea. Elemental sulphur is the electron donor in various sulphur-oxidation pathways in aerobic lithotrophic species (reviewed in, e.g., [1–3]) and is the electron acceptor in respiratory chains of anaerobic heterotrophic and autotrophic micro-organisms [4]. Many studies have been conducted to elucidate the mechanisms of inorganic sulphur compound oxidation. In most cases, water-soluble substrates such as thiosulphate or tetrathionate were used (e.g. [3,5,6]). However, much less is known about the oxidation of the virtually insoluble elemental sulphur (5 μg/l of water at 25 °C [7]).

Soluble glutathione-dependent and periplasmatic sulphur oxygenases have been identified in the mesoacidophilic bacteria such as *Acidithiobacillus ferrooxidans* and *Acidithiobacillus thiooxidans*; however, there is not much known about the biochemistry and molecular biology of the enzymes (e.g. [8–10]). More is known about the periplasmatic multi-enzyme Sox (sulphur-oxidizing) system of the neutrophilic, facultatively lithoautotrophic bacterium *Paracoccus pantotrophus* GB17 and other species [1,5,11,12]. This system catalysed the thiosulphate-, sulphite-, sulphur- and hydrogen sulphide-dependent cytochrome *c* reduction *in vitro*. These findings, together with the analysis of genetic and genomic data, led to the suggestion that we observe the "emergence of a common mechanism" [3] of the oxidation of inorganic sulphur compounds by the Sox system in many different neutrophilic bacteria; however, Sox proteins or genes have not been found in the acidophiles. According to this model, the oxidation of these compounds occurs completely in the enzyme-bound state without any free intermediates.

Less is known about sulphur-oxidation pathways in the Archaea. A soluble SOR (sulphur oxygenase reductase) was purified from aerobically growing cells of the thermoacidophilic crenarchaeote *Acidianus ambivalens*, which catalysed the simultaneous oxidation and reduction of elemental sulphur in the presence of oxygen, with sulphite, thiosulphate and hydrogen sulphide as products [13]. Cofactors or an external electron donor for sulphur reduction were not required, and the two enzyme activities could not be separated. The enzyme consisted of a multimer of identical subunits. Its molecular mass deduced from the gene sequence was 35 188 Da (the N-terminal methionine is cleaved off in the wild-type enzyme [14]). As the SOR was the only sulphur-oxidizing enzyme found in *Acidianus ambivalens*, it was thus assumed that the enzyme catalysed the initial step of the sulphur-oxidizing pathway in this organism. Considering that its cytoplasmic location does not contribute to the formation of a transmembrane proton gradient, it is likely that it provides soluble precursors for membrane-bound enzymes such as a thiosulphate:quinone oxidoreductase [14a].

A similar enzyme had been purified from a phylogenetically uncharacterized isolate tentatively termed "*Sulfolobus brierleyi*". A moderate ^{18}O incorporation into sulphite was demonstrated;

---

however, a sulphur reductase activity was not reported [15]. In addition, a *sor* gene from *Acidianus* sp. strain S5 was cloned and expressed heterologously in *Escherichia coli* [16]. The three enzymes had comparable properties [17,18]. So far, little is known about the cofactor content, the reaction mechanism, the number of subunits and the exact quaternary structure of the SOR.

In the present study, we show that a low-potential mononuclear non-haem iron centre is present in the *Acidianus ambivalens* SOR and that it plays an essential role in catalysis. We also show that the purified complex is a large oligomer in solution, having a ferritin-like assembly. We propose that the sulphur-oxidation pathway in *Acidianus ambivalens* is distinctly different from the Sox pathway found in numerous mesophilic aerobic and anaerobic oxidizers of sulphur compounds.

EXPERIMENTAL

Heterologous gene expression and purification of recombinant SOR from *E. coli*

The *sor* gene was amplified from genomic *Acidianus ambivalens* DNA using the primers SoroN (5′-TAGACATCTAGATAACG-AGGGCAAAAAATGCCGAAACCATACGT-3′) and SoroC (3′-AGAAAAAGCTTAAGCGCTTTGTTCGTTTAAATATTCTC-5′). The product was digested with *Xba*I and *Eco*47III and ligated into the pASK 75-plasmid [19] double-digested with the same enzymes, resulting in a gene fusion encoding a C-terminal ten-amino-acid streptavidin tag. The construct was transformed into *E. coli* BL 21 Codon plus cells (Stratagene). Attempts to construct an expression plasmid with the wild-type sequence failed.

The expression of the *sor* gene was induced by addition of anhydrotetracycline (200 μg/l of culture) to a 15 l culture growing at 37 °C at a D_{600} of 0.8 and incubated overnight after induction with vigorous aeration. The harvested cells (77 g wet mass) were resuspended in 770 ml of 100 mM potassium phosphate (KP$_i$) buffer, pH 8, containing 1 % (v/v) Tween 20 and 50 μM EDTA. The cells were disrupted in a cell mill (Vibrogen V/3) by shaking with glass beads for 20 min. After removal of the glass beads by filtration, the crude extract was centrifuged at 48 000 *g* for 20 min. The supernatant (700 ml, 3.5 g of protein) containing the soluble SOR was heat-treated for 45 min at 75 °C to precipitate heat-labile *E. coli* proteins and centrifuged again under the same conditions. The supernatant obtained was dialysed against 20 mM Tris/HCl, pH 7.5. A total volume of 100 ml of the dialysed protein fraction was applied to a DEAE-Sepharose fast-flow column (60 ml bed volume; all columns and column materials were from Amersham Biosciences) and eluted with an increasing gradient of NaCl in the same buffer. The recombinant SOR eluted at 150 mM NaCl. Active fractions were pooled. The protein was sedimented by ultracentrifugation at 42 000 rev./min (Beckman 45 Ti rotor) for 16 h. The pellet was resuspended in 50 mM Tris/HCl, pH 7.5, and was frozen at −20 °C.

Unfolding and refolding of SOR from inclusion bodies

The pellet of the crude *E. coli* extract containing large amounts of inclusion bodies was resuspended in KP$_i$ buffer, pH 8, containing 1.5 % sodium deoxycholate, 1 M urea, 10 % (v/v) glycerol and 2 mM EDTA, by sonication for 5 min (Branson Sonifier II) and was washed four times in the same buffer. The washed inclusion body fraction (approx. 5 g) was resuspended in 50 ml of 8 M urea containing 100 μM ferric citrate and 30 mM dithiothreitol. After denaturation at 60 °C for 1 h, the solution was centrifuged at 48 000 *g* for 30 min to remove particulate material. Refolding of the SOR was performed aerobically at 4 °C by a two-step

dialysis against 50 mM Tris/HCl, pH 7.2, containing 2 mM 2-mercaptoethanol and 100 μM ferric citrate, with 2 M urea in the first step, and no urea in the second step. Residual ferric citrate and 2-mercaptoethanol were removed from the refolded enzyme preparation in another dialysis step against 50 mM Tris/HCl, pH 7.5. The protein solution was centrifuged under the same conditions to remove precipitated protein and subjected to the SOR activity assay.

Alternatively, unfolded inclusion bodies were dialysed three times against 8 M urea without ferric citrate to remove residual iron from the samples. The samples were subsequently refolded with 0, 10 or 100 μM ferric citrate as described above.

Denaturant-induced protein unfolding

Stock solutions of GdmCl (guanidinium chloride) and urea for protein unfolding of the soluble recombinant SOR were prepared following published recommendations [20], and final molarities were calculated from refractive index measurements. Denaturation curves were determined at 25 °C using wild-type SOR in 50 mM Tris/HCl buffer, pH 7, at a final concentration of 0.01 mg/ml. The unfolding process was monitored by fluorescence spectroscopy monitoring tryptophan emission (300–450 nm; excitation, 292 nm; 1 cm cell) on a Varian Eclipse fluorimeter. The spectroscopic data were processed in order to determine the average emission wavelength at each denaturant concentration [21], and the resulting unfolding transitions were analysed using a two-state model, allowing for the calculation of thermodynamic parameters [22]. Direct fits to the experimental unfolding curves were performed using the following expression:

$$Y_{obs} = Y_U - Y_F \cdot [\exp(\{\Delta G_U(H_2O) - m \cdot [\text{denaturant}]\}/RT)]/$$
$$[1 + (\exp(\{\Delta G_U(H_2O) - m \cdot [\text{denaturant}]/RT\}))]$$

where Y_{obs}, Y_U and Y_F are the observed spectroscopic signal, denaturant protein baseline and folded protein baseline respectively, m is a constant of proportionality, R is the gas constant and T is the absolute temperature (in K). The transition midpoints were calculated as $\Delta G_U(H_2O)/m$ or by direct inspection of the transitions.

For the determination of the molecular masses of unfolding intermediates and of the partially unfolded proteins, 200 μl portions of a 1 mg/ml solution of recombinant SOR were dialysed against 0–8 M urea in 20 mM KP$_i$ buffer, pH 6.5, at room temperature (22–25 °C) for 48–72 h. Dialysed protein fractions (200 μl) were applied to a Superose 6 HR 10/30 gel-permeation column equilibrated with 20 mM Tris/HCl buffer, pH 7.5, and 150 mM NaCl not containing any urea. Identically treated samples (45 μg each) were separated by Blue-native (BN) PAGE [23] by applying a 4–15 % polyacrylamide gradient in 14 cm × 14 cm × 0.15 cm gels, run in an SE400 vertical electrophoretic chamber. The molecular masses of the SOR bands were calculated from retardation coefficients after electrophoresis on BN gels of different polyacrylamide concentrations (Ferguson plot; 5.5, 6.5, 7.5, 8.5, 9.5 and 10.5 % polyacrylamide; Sigma Technical Bulletin No. MKR-137 available at http://www.sigmaaldrich.com/sigma/bulletin/mwnd500bul.pdf). The MW ND-500 kit, containing lactalbumin, carbonic anhydrase, ovalbumin, BSA and urease, was used for standards, in addition to catalase, ferritin and thyroglobulin (all from Sigma).

Purification of wild-type SOR from *Acidianus ambivalens*

Acidianus ambivalens DSM 3772 was grown aerobically according to published procedures [24,25]. A novel protocol for the

preparation of wild-type SOR from *Acidianus ambivalens* was developed. Crude-extract preparation and sucrose density-gradient centrifugation were performed as described previously [13]. Active fractions were combined and dialysed against 0.5 M $(NH_4)_2SO_4$ and 20 mM Tris/HCl, pH 7.5. The protein solution was loaded on a phenyl-Sepharose column, equilibrated with the same buffer, and eluted with a decreasing $(NH_4)_2SO_4$ gradient in a HiLoad system 26/10. The SOR was eluted at around 50 mM $(NH_4)_2SO_4$ and was pooled according to activity. The active fractions were combined, dialysed against 20 mM Tris/HCl, pH 7.5, applied to a DEAE-Sepharose fast-flow column as described above, and eluted with an increasing NaCl gradient in the same buffer. The SOR eluted at around 150 mM NaCl. The active fractions were pooled and concentrated using a Jumbosep ultrafiltration unit (cut-off size 30 kDa) and stored at $-20\,°C$.

The purified proteins from the purification and refolding protocols were finally run over a Superose 6 HR 10/30 gel-permeation column in 20 mM Tris/HCl, pH 7.5, and 150 mM NaCl. Thyroglobulin, ferritin, catalase, aldolase, chicken albumin and carbonic anhydrase (Sigma) were used for calibration and determination of the holoenzyme and subunit masses.

Biochemical and analytical methods

The SOR activity assay was performed aerobically at $85\,°C$ in 70 mM Tris/HCl, pH 7.2, containing 0.1 % (v/v) Tween 20, as previously described [13]. After incubation for different time intervals, the products were determined colorimetrically. It was assumed that sulphite and sulphide are the sole primary products and that thiosulphate resulted from a non-enzymic reaction between sulphite and sulphur [13]. One unit of enzyme activity was defined as the formation of 1 μmol of sulphite plus thiosulphate (oxygenase reaction) or 1 μmol of hydrogen sulphide (reductase reaction) per min. The reaction velocity was calculated from the linear increase of product concentrations.

A concentration of 0.5 % (v/v) CHAPS was used for the K_m and k_{cat} determinations, and the assay temperature was lowered to $65\,°C$ to slow down the reaction velocity. The determinations of the two K_m values for sulphur were performed using the rate of formation of the products sulphite and sulphide separately.

Enzyme assays for inhibition studies were usually performed with EDTA-washed sulphur prepared as follows: 50 g of sulphur (Merck) was dispersed in 500 ml of enzyme buffer with 10 mM EDTA by sonication for 5 min with a Branson Sonifier (II) followed by centrifugation at 48 000 *g* for 15 min three times each. EDTA was removed by washing the sulphur over a filter with 5 litres of double-deionized water. Potassium tetrathionate and unwashed sulphur were alternatively used as substrates. The following reagents were tested for potentially inhibitory effects: EDTA, $ZnCl_2$, $CaCl_2$, $MgCl_2$, Fe(III) citrate, $(NH_4)_2Fe(SO_4)_2$ and sodium citrate. The reagents were added to the enzyme-containing assay mixture. After 30 min of incubation at room temperature, the pH was readjusted to 7.2 with a solution of 1 M Tris base. Raising the temperature to $85\,°C$ started the enzymic reaction. An enzymic reaction without inhibitor and a non-enzymic reaction with inhibitor, but without SOR, were used as controls. The interference of the substances with the colorimetric assays was determined by adding mixtures of sodium sulphite, sodium thiosulphate and sodium sulphide (50 μM each) in enzyme buffer to the colorimetric assay reactions with inhibitor concentrations equal to the ones used in the enzymic assays.

The protein concentration was determined by the Bradford [26] or BCA (bicinchoninic acid) methods [27]. The protein concentration of pure SOR preparations was determined by measuring the A_{280} using the calculated molar absorption coefficient, $\varepsilon =$ 57 840 $M^{-1} \cdot cm^{-1}$ (from sequence). Sample purity was assessed using SDS/10 % polyacrylamide gels [28] and visualized with colloidal Coomassie Blue (Roti-Blue; Roth, Karlsruhe, Germany). The iron content was determined by the 2,4,6-tripyridyl-1,3,5-triazine method [29].

Spectroscopic methods and redox titration

UV/visible spectra were recorded at room temperature in a Shimadzu spectrophotometer. CD spectra were obtained by use of a Jasco J810 spectropolarimeter. The CD spectra were obtained using a cuvette of 0.2 cm path length and at a scanning speed of 50 nm/min and a bandwidth of 2 nm. Scans were collected at 1 nm intervals with a response time of 0.25 s and accumulated ten times. The CD spectra were corrected by subtracting the spectrum of the buffer solution (20 mM KP_i, pH 6.5). The spectra between 187 and 250 nm were used to calculate the α-helical and β-sheet content of the native, recombinant and refolded SOR preparations using the programs CONTINLL and SELCON3 included in the CDPro software package and a reference protein set containing 37 proteins [30].

EPR spectra were recorded on a Bruker ESP380 spectrometer, equipped with an ESR 900 continuous flow helium cryostat. *Acidianus ambivalens* wild-type SOR was titrated anaerobically in 50 mM KP_i, pH 6.5, by sequential addition of alkaline buffered sodium dithionite and continuously flushing the cell with argon. EPR samples were withdrawn at the desired potential and were immediately frozen in liquid nitrogen. The intensity of the $g = 4.3$ resonance was followed as a function of the reduction potential of the solution. The following compounds were used as redox mediators (40 μM each, E'_0 in parentheses): 1,2-naphthoquinone-4-sulphonic acid (215 mV); 1,2-naphthoquinone (180 mV); trimethylhydroquinone (115 mV); phenazine methosulphate (80 mV); phenazine ethosulphate (55 mV); Methylene Blue (11 mV); Indigo Tetrasulphonate (-30 mV); resorufin (-51 mV); Indigo Trisulphonate (-70 mV); Indigo Disulphate (-182 mV); 2,5-hydroxy-*p*-benzoquinone (-130 mV); 2-hydroxy-1,4-naphthoquinone (-152 mV); anthraquinone-2-sulphonate (-225 mV); phenosafranine (-255 mV); safranine (-280 mV); Neutral Red (-325 mV); Benzyl Viologen (-359 mV); and Methyl Viologen (-446 mV). A platinum and a silver/silver chloride electrode were used, calibrated against a saturated quinhydrone solution at pH 7.0. The reduction potentials are quoted in respect to the standard hydrogen electrode.

Electron microscopy

SOR samples were diluted to a protein concentration of 0.1 mg $\cdot$ ml^{-1}, applied to glow-discharged carbon-coated copper grids and negatively stained with 2 % uranyl acetate. Electron micrographs were taken using a slow-scan CCD (charge-coupled device) Tietz camera mounted to a Philips CM 12 electron microscope operated at 120 kV. Image analysis by single particle averaging was performed as described previously [31,32] using the EM program [33] and the SEMPER software [34].

Sequence analysis

The amino acid sequence of the *Acidianus ambivalens* SOR was compared with sequences in the public databases using different BLAST tools for the identification of homologues. SOR sequences were retrieved and aligned using the alignment tools PileUp, ClustalW and HmmerAlign included in the Wisconsin package (Accelrys). The PredictProtein server and the programs within were used to predict secondary-structure elements (http://cubic.bioc.columbia.edu/predictprotein/). The number of atoms
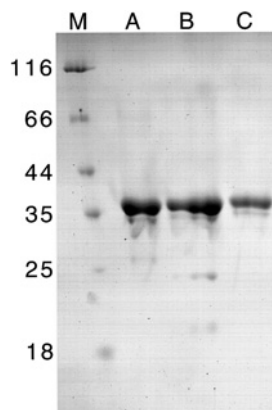
Figure 1   SDS/10 % polyacrylamide gel stained with colloidal Coomassie Blue with purified wild-type and recombinant SOR

(**A**) Wild-type SOR (6.3 μg of protein), (**B**) recombinant SOR refolded from inclusion bodies (6.3 μg of protein) and (**C**) recombinant SOR purified from the soluble *E. coli* fraction (4.2 μg of protein). M, molecular mass markers (in kDa).

was calculated using ProtParam (http://www.expasy.org/tools/protparam.html). The *Acidithiobacillus ferrooxidans* genome was queried at the TIGR web server (http://www.tigr.org).

RESULTS

Heterologous gene expression in *E. coli* and purification of recombinant and wild-type SOR

A *sor* gene expression plasmid was constructed with the open reading frame fused to the streptavidin tag at the 3′ end. Soluble *E. coli* extracts harvested 20 h after induction of *sor* gene expression showed an enzyme activity of 464 m-units of oxidase/mg of protein and 145 m-units of reductase/mg of protein. From the extract (3.5 g of protein), 120 mg of SOR was isolated. The specific activity of the purified recombinant soluble enzyme was 2.82 units of oxygenase/mg of protein and 0.66 unit of reductase/mg of protein, at 85 °C.

At 2 h after induction, the occurrence of the first inclusion bodies was observed microscopically. Approx. 80 % of the protein in the pellet fraction after cell lysis consisted of SOR (results not shown). After extensive washing, the yield was 2 g of inclusion body fraction (wet mass)/l of *E. coli* culture. The inclusion body fraction was unfolded in 8 M urea and refolded in a two-step dialysis. The activities of the recombinant enzyme from inclusion bodies were up to 5.98 units of oxygenase/mg of protein and 1.35 units of reductase/mg of protein, when refolded in the presence of ferric iron (see below).

Wild-type SOR (10.5 mg) was purified using a novel protocol from 175 mg of soluble *Acidianus ambivalens* cell extract via sucrose density-gradient centrifugation and two chromatographic steps. The specific activities were 2.96 units of oxygenase/mg of protein and 0.60 unit of reductase/mg of protein. SDS/PAGE showed that the different procedures yielded pure enzyme (Figure 1). Apart from the major 36 kDa band, two faint low-molecular-mass bands were observable, but N-terminal sequencing revealed that they were proteolysis products of the 36 kDa subunit (results not shown).

SOR is a multimeric protein composed of dimer building blocks

The apparent molecular masses of wild-type, recombinant soluble and refolded holoenzymes determined by gel-permeation chromatography were approx. 550 kDa, showing that the enzyme preparations from *E. coli* adopted a near-native state. Recombinant SOR preparations were dialysed extensively against different urea concentrations and were analysed with gel-permeation chromatography. An additional peak corresponding to a molecular mass of 72 kDa equivalent to a SOR dimer appeared in preparations containing 3 M urea or above, whereas the holoenzyme peak decreased with increasing urea concentration (Figure 2A). A peak corresponding to 35 kDa or the SOR monomer appeared in preparations dialysed against 6 M urea or above, whereas the dimer and holoenzyme peaks diminished. The 72 kDa peak was also observed in varying intensities in samples of refolded and wild-type SOR not treated with any urea (results not shown).

SOR activity was observed with up to 5 M urea, but not above (Figure 2B). Comparative analysis of all peak fractions by SDS/PAGE under reducing and non-reducing conditions showed only the 36 kDa band; the absence of a dimer band indicated that inter-subunit disulphide bridges were not present (results not shown).

Identically treated samples separated with non-denaturing BN gels showed that the holoenzyme band dominated in samples dialysed against 0–3 M urea (Figures 2C and 2D). Intensely stained bands corresponding to monomer and dimer sizes and in lesser intensity to higher oligomers were seen in samples dialysed against 6 M urea and above. In the 2–4 M urea lanes, a faint ladder of partially denatured protein was observed. A dominant dimer band appeared in these lanes, which had a different migration pattern compared with those of the fully denatured samples (Figure 2D). The determination of the apparent molecular mass of the holoenzyme by BN PAGE gave a value of 732 kDa.

Conformational stability of *Acidianus ambivalens* SOR

The conformational stability of wild-type *Acidianus ambivalens* SOR was investigated by inducing unfolding at neutral pH using the denaturants GdmCl and urea. Protein unfolding was monitored by following the emission fluorescence spectrum of tryptophan residues, which were used as intrinsic probes for protein stability. The reversible denaturation curves were found to have midpoints at 3.4 M GdmCl and 5.9 M urea (Figure 3), when analysed using a two-state model for the folding/unfolding reaction. The protein apparent folding free energy in water was determined to be approx. 5 kcal · mol^{-1} (1 kcal = 4.184 kJ), at pH 7 (Figure 3, see legend for details). This low value is explained by the fact that, although the native conformation is essential for activity, its stability in respect to the unfolded state is very low, typically ranging from 5 to 15 kcal · mol^{-1} [22]. Dialysis of the unfolded protein in the presence of high denaturant concentrations restored the initial emission spectra, indicating that the observed chemical-denaturant-induced unfolding transition is reversible. This was corroborated further by the fact that active SOR could be obtained from inclusion bodies dissolved in 8 M urea.

Electron microscopy reveals a globular multimer

In transmission electron micrographs of negatively stained wild-type and SOR preparations, globular particles of 15.5 nm diameter were visible [13]. The inner core appeared densely stained. Electron micrographs of recombinant protein gave essentially the same results (Figures 4A and 4B). Single particle averaging of individual wild-type particles revealed two distinct subpopulations occurring in similar amounts. One subpopulation showed a 4-fold (Figure 4C), the other a 2- or 3-fold symmetry axis (Figure 4D), indicating that the holoenzyme is a highly symmetrical particle.
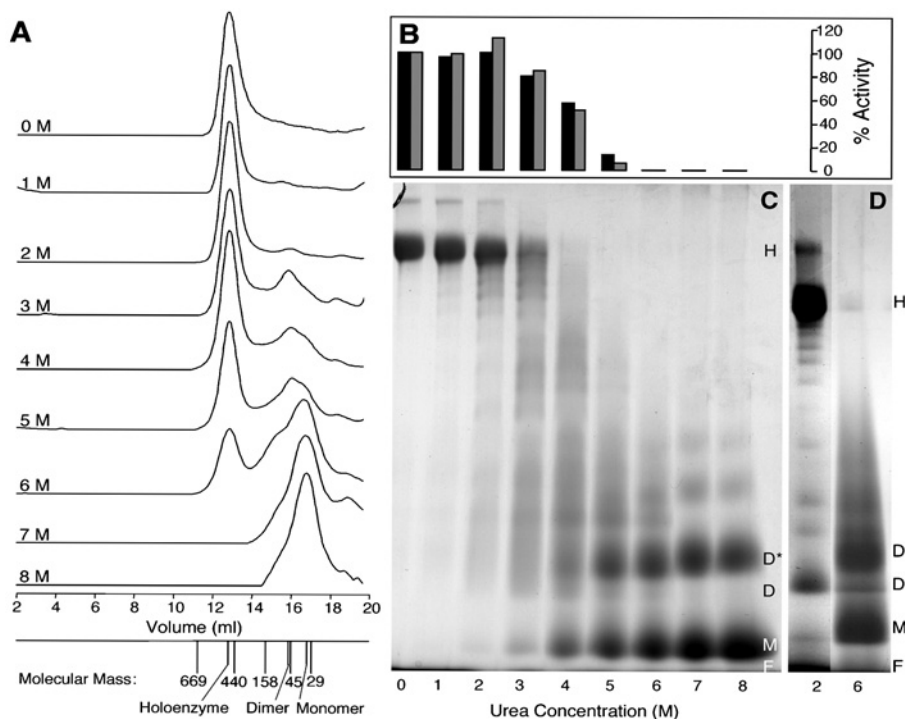
Figure 2   Gel permeation chromatography, enzyme activity and BN gels of recombinant soluble SOR dialysed against various concentrations of urea as described in the Experimental section

(**A**) Merged gel permeation chromatograms given with the respective urea concentration. The protein peaks were monitored by measuring the A_{280}. The elution volumes of thyroglobulin, ferritin, aldolase, chicken albumin and carbonic anhydrase are given with their molecular masses, together with the holoenzyme, dimer and monomer peaks. (**B**) Relative specific activities of the SOR fractions after dialysis against different urea concentrations as indicated below the gel (**C**). The oxygenase (black) and reductase activities (grey) of the 0 M urea control were each set to 100 %. (**C**) BN gradient gel of SOR preparations dialysed against different urea concentrations re-stained with colloidal Coomassie Blue after electrophoresis. (**D**) As in (**C**) showing a ladder of oligomers of the partially denatured enzyme. H, holoenzyme; D*, dimer denatured; D, dimer; M, monomer; F, migration front.

Secondary-structure analysis reveals an almost equal distribution of α-helices and β-sheets

CD spectra of the different preparations were rather similar, with minima around 220 and 207 nm, and a maximum around 195 nm, and minor differences in the molar ellipticity at 187–197 nm and at 220 nm (Figure 5). Secondary-structure analysis of the wild-type SOR spectrum resulted in $23.8 \pm 1.5\%$ α-helix and $23.4 \pm 0.8\%$ β-sheet content. The recombinant and refolded preparations showed an α-helical content of $25.2 \pm 0.6\%$ and $25.7 \pm 0.9\%$ and a β-sheet content of $26.2 \pm 0.5\%$ and $24.2 \pm 0.2\%$ respectively. The average length of the helices predicted was nine amino acids. Secondary-structure prediction programs gave 29 % α-helical and 27 % β-sheet content, which is in good agreement with those calculated from the CD spectra.

Iron is essential for SOR activity

The determination of the iron content of wild-type SOR preparations resulted in a ratio of 1.0 iron atom per subunit of SOR. For the two recombinant SOR preparations, ratios of 2.2 (soluble) and 1.4 (refolded) iron were calculated per subunit. When no ferric citrate was added to the unfolding and refolding buffers and the unfolded protein solution was extensively dialysed against 8 M urea before refolding to remove residual iron, the specific activities were 0.006 units of oxygenase/mg of protein and 0 unit of reductase/mg of protein. A parallel sample, refolded in the presence of 10 μM ferric citrate, had specific activities of 0.29 unit of oxygenase/mg of protein and 0.06 unit of reductase/

mg of protein, whereas the activities were 5.98 units of oxygenase/mg of protein and 1.35 units of reductase/mg of protein, when refolded in the presence of 100 μM ferric citrate.

EPR spectroscopy reveals a mononuclear non-haem iron centre

The UV/visible spectra of SOR did not show any feature besides the protein absorption at 280 nm in the reduced or oxidized state (results not shown). EPR spectroscopy performed at liquid-helium temperature of wild-type SOR showed an isotropic resonance at $g = 4.3$ in the 'as prepared' state, consistent with the presence of a mononuclear non-haem iron centre in the ferric high-spin state and a rhombicity of 0.33 (Glu/Asp; Figure 6). Both recombinant and refolded proteins showed the same type of signal, although with a higher intensity. Adequate controls showed that the observed signal was from the enzyme and not from the buffers used.

The intensity of the $g = 4.3$ signal decreased upon incubation with elemental sulphur at 80 °C up to 20 min. The signal disappearance was not reversible after the SOR had been washed with oxidized buffer following the reaction. This observation suggests that an intermediate may remain bound to the metal reaction site upon catalysis. The E'_0 of the mononuclear iron centre was determined in an EPR-monitored redox titration experiment to be -268 mV (Figure 6, inset).

Catalytic properties of wild-type and recombinant SOR

The apparent K_m values for sulphur, determined with the oxygenase and the reductase reaction separately at 65 °C, were
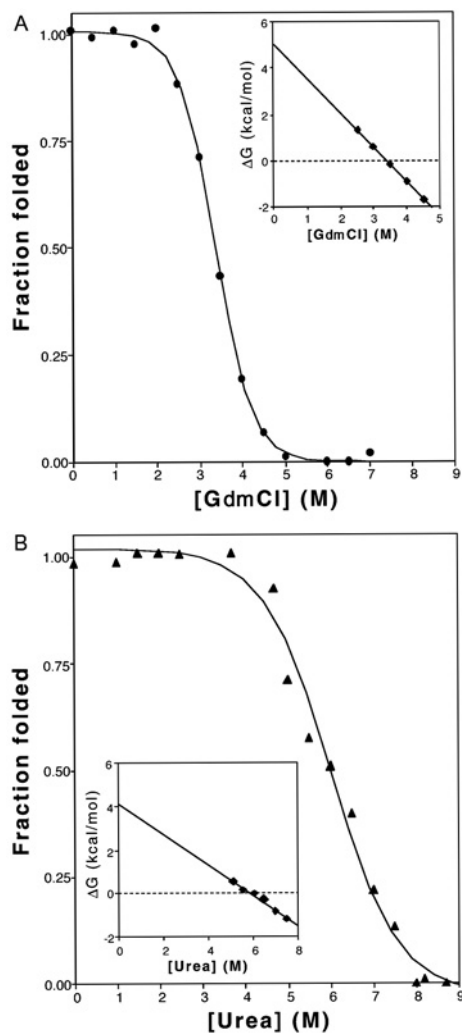
Figure 3   GdmCl (A) and urea (B) denaturation curves

The solid lines are a least-squares analysis fit of the experimental data to a two-state F $\leftrightarrow$ U model yielding the following parameters: $\Delta G(H_2O) = 5.04$ kcal/mol, $m = 1.49$ kcal/mol per M and $[GdmCl]_{1/2} = 3.38$ M (**A**); $\Delta G(H_2O) = 4.13$ kcal/mol, $m = 0.7$ kcal/mol per M and $[urea]_{1/2} = 5.89$ M (**B**). It should be noted that m depends on the amount of polypeptide chain that is exposed to solvent upon unfolding, and thus varies with denaturants [22]. The insets are plots of the variation of ΔG_U in the transition region as a function of denaturant concentration, according to the $\Delta G_U = \Delta G(H_2O) - m \cdot$ [denaturant] equation.

Figure 4   Electron micrographs of negatively stained SOR, and image reconstruction

(**A**, **B**) Micrographs of wild-type and recombinant SOR respectively; the bar represents 100 nm; (**C**, **D**) results of single particle averaging of SOR particles with 2-fold and 3-fold symmetry axis respectively.
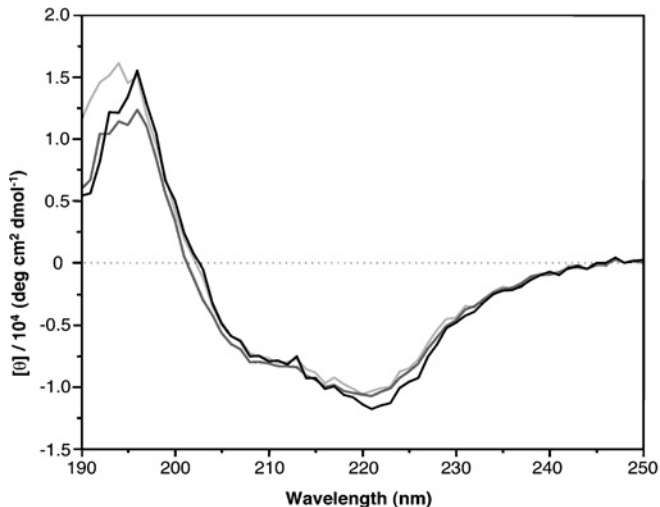
Figure 5   CD spectra of wild-type (light grey), recombinant soluble (dark grey) and recombinant refolded (black) SOR

All the CD spectra were displayed relative to the buffers used. The y-axis represents the mean residue molar ellipticity obtained using the protein concentration, the path length and the number of protein residues for calculation (wild-type, 308; recombinant, 318).

23 mM and 13 mM respectively, calculated on the basis of S°, not S$_8$. The k_{cat} values were 2.2 s^{-1} and 0.1 s^{-1} (oxygenase and reductase respectively).

Several substrates and potential inhibitors were tested for their effects on SOR activity (Table 1). The SOR was not active with tetrathionate. Metal chelators, such as EDTA and sodium citrate, were not inhibitory even in concentrations as high as 100 mM in the case of EDTA. In contrast, EDTA showed a slight stimulatory effect (Table 1), which was also seen in enzymic assays with partially denatured SOR (results not shown).

We tried to determine whether or not the EDTA effect was due to the binding of potentially inhibitory bivalent cations. Ca^{2+} and Mg^{2+} had no effect on the enzyme activity (Table 1), whereas Zn^{2+} showed a strong inhibition, as observed previously [13]. The effect of Zn^{2+} was abolished when EDTA was also added to the assay mixture. To determine whether inhibitory traces of transition metals i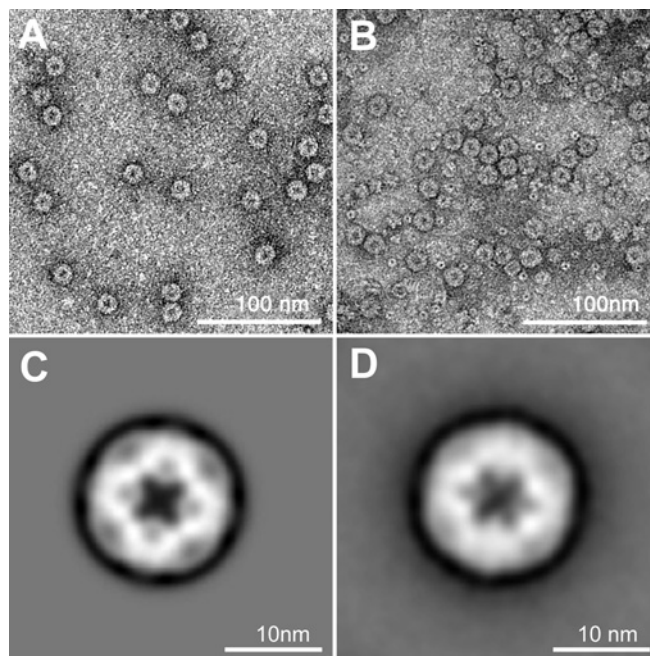n the substrate sulphur caused the stimulatory effect of EDTA, sulphur was washed with EDTA-containing buffer. The incubation of washed sulphur with additional EDTA in the assay buffer resulted in the same increase in activity as determined with the unwashed sulphur (Table 1). The addition of low amounts of Fe^{2+} or Fe^{3+} neither inhibited nor increased the activity in low concentrations, but interfered with the colorimetric assays, thus preventing the use of higher concentrations.

Figure 6   EPR spectrum of wild-type *Acidianus ambivalens* SOR

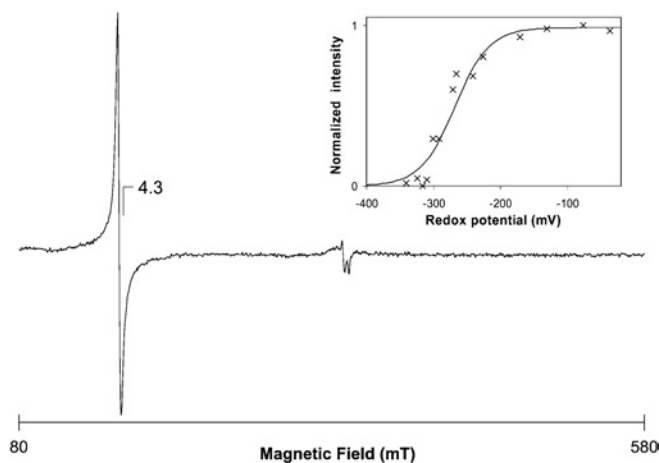Temperature, 4.6 K; protein concentration, 226 μM; microwave power, 2.4 mW; modulation amplitude, 1 mT. Inset, redox titration of the SOR mononuclear iron centre. The normalized intensities of the $g = 4.3$ resonance are plotted against the reduction potential. The line represents a Nernst equation for a one-electron step transition, with an $E_m = -268$ mV.

Table 1   Effects of various substrates and reagents on SOR activity

The substrate (sulphur) concentration was 78 mM.

Substrate	Reagent	Reagent concentration (mM)	Activity (%) Oxygenase	Reductase
Sulphur (S$_8$)	–	–	100	100
	EDTA	1	127	143
	EDTA	10	150	141
	EDTA	50	160	108*
	EDTA	100	134	13*
	Ca^{2+}	1	82	101
	Mg^{2+}	1	110	92
	Sodium citrate	1	103	85
Sulphur (S$_8$), EDTA-washed	–	–	104	94
	EDTA	10	147	124
	Zn^{2+}	0.5	5	16
	EDTA/Zn^{2+}	1/0.5	114	86
	Fe(III) citrate	0.1	102	19*
	Fe(III) citrate	0.01	96	1*
	(NH$_4$)$_2$Fe(SO$_4$)$_2$	0.1	105	150
	(NH$_4$)$_2$Fe(SO$_4$)$_2$	0.01	110	90
No sulphur	K$_2$ Tetrathionate	10	0	0

* Interference with the colorimetric assays.

Comparison of SOR amino acid sequences

Homologous *sor* genes were also found in BLAST searches in the genomes of the archaea *Sulfolobus tokodaii*, *Ferroplasma acidarmanus* and the hyperthermophilic bacterium *Aquifex aeolicus*; in addition, the *sor* gene from *Acidianus sp.* strain S5 had already been described [16]. The pairwise similarities of the deduced amino acid sequences compared with the *Acidianus ambivalens* enzyme ranged from 39 % (*Aquifex aeolicus*) to 88 % (*Acidianus* S5; Figure 7). Extensive database searches using PSIBLAST and other search tools did not provide any further motifs or significant similarities to other proteins. No similar gene was found when searching the genome sequence of the sulphur- and iron-oxidizing mesophilic bacterium *Acidithiobacillus ferrooxidans*.

DISCUSSION

In the present paper, we report a biochemical and functional characterization of the recombinant and the wild-type *Acidianus ambivalens* SOR, focusing on the enzymic activity, on the first description of one of the redox active centres, and on evidence regarding the quaternary structure of the enzyme.

The specific activities of several preparations of recombinant, refolded and wild-type SOR were comparable, as well as the results of the electron microscopy, the gel-permeation chromatography, and the CD and EPR spectra, suggesting that: (i) the recombinant enzyme possess similar properties to those of the wild-type enzyme, (ii) the purification and refolding procedures gave reliable results, and (iii) the C-terminal ten-amino-acid streptavidin tag did not impair the function of the enzyme.

The K_m of 18 mM (average of the oxygenase and reductase tests), and the k_{cat} of 2.2 s^{-1} and 0.1 s^{-1} respectively, suggest a low substrate affinity and enzyme velocity. A similar K_m of 50 mM had been reported for the oxygenase reaction of the "*Sulfolobus brierleyi*" enzyme [15]. A possible explanation for the unfavourable values lies in the poor solubility of sulphur [7] and, therefore, low substrate availability, despite the large excess in the assay thus preventing the enzyme from reaching maximal velocity.

The results of the refolding experiments with different iron concentrations showed that its presence was essential for the catalytic activity of the refolded SOR. Slightly higher iron/subunit ratios were observed in the recombinant enzyme preparations as compared with the wild-type enzyme; however, the strong EPR signal of the oxidized 'as prepared' SOR showed that iron is probably present in a mononuclear centre in each subunit. The lack of any absorbance of the enzyme in the UV/visible spectrum, besides the absorption at 280 nm, points to histidine and/or carboxylate, but not cysteine, ligation of the iron, as observed in many oxygenases with mononuclear or binuclear non-haem iron centres (e.g. [35]).

The reduction potential of the iron is, to our knowledge, the lowest observed for mononuclear centres ($E_m = -268$ mV). Other proteins known to harbour colourless mononuclear non-haem iron centres show clearly positive E_0' values, typically ranging from $+200$ to $+600$ mV (e.g. [36–39]). This low reduction potential most probably originates from a different protein environment around the iron centre. Nevertheless, the reduction potential is low enough to explain the observed reductase activity of the enzyme (E_0' for H$_2$S/S$^\circ = -270$ mV [40]).

A tight binding of the iron is suggested by the observation that EDTA was not inhibitory at all; in contrast, it stimulated the enzyme activity even in assays with partially denatured enzyme (results not shown). The removal of potentially inhibitory traces of transition metals bound to the SOR in the 'as isolated' state could be a reason for this effect. This explanation is supported further by the observations that: (i) the specific activities of the enzyme refolded from inclusion bodies were often higher than those obtained after regular purification, (ii) the inhibitory effect of Zn^{2+} could be reversed by the addition of EDTA to the reaction mixture, and (iii) the EDTA effect could not be explained by the presence or absence of Mg^{2+} and Ca^{2+}, since those metals did not have any effect (Table 1).

SOR sequence analysis and active-site predictions

Four of the five SOR sequences had been tentatively grouped in a Pfam B domain (Pfam-B_28360; http://www.sanger.ac.uk/Software/Pfam). No overlap with other domains was detected. Similarly, our analyses did not provide evidence that the SORs are phylogenetically related to any other enzyme family, regardless
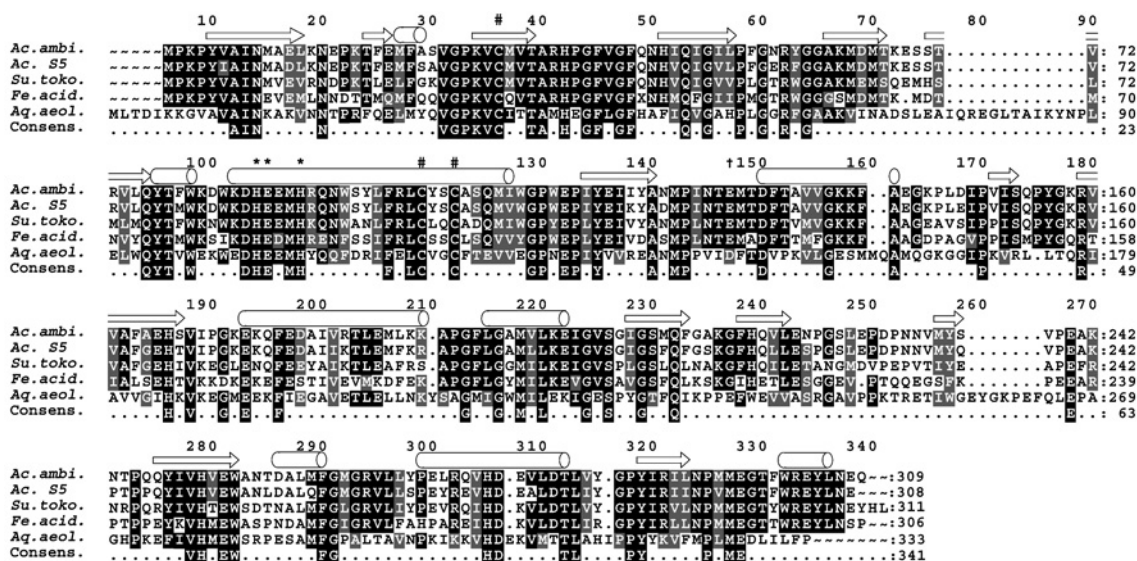
```
              10        20        30      #  40        50        60        70        80        90
Ac.ambi.  -----MPKPYVAINMABLKNEPKTFEMFASVGPKVCMVTARHPGFVGFQNHIQIGILPFGNRYGGAKMDMTKESST.............V: 72
Ac. S5    -----MPKPYIAINMADLVRNDPKTFEMFSAVGPKVCMVTARHPGFVGFQNHVQIGVLPFGERFGGAKMDMTKESST.............V: 72
Su.toko.  -----MPKPYVAINMVEVRNDPKTLELFGKVGPKVCMVTARHPGFVGFQNHVQIGVVPLGTRWGGAKMEMSQEMHS.............L: 72
Fe.acid.  -----MPKPYVAINEVEMLNNDTTMOMFQQVGPKVCQVTARHPGFVGFXNHMQFGIIPMGTRWGGGSMDMTK.MDT.............: 70
Aq.aeol.  MLTDIKKGVAVAINKAKVNNTPRFQELMYQVGPKVCITTARHPGFHAFIQVGAHKLGGRFGGAAKVINADSLEAIQREGLTAIKYNPL: 90
Consens.  .....AIN...VGPKVC..TA.H.GF.GF......Q.G..F.G.R.G.............................: 23

              100    ** *        #  #   130      140    †150        160      170        180
Ac.ambi.  RVLQYTWKDWKDHEEMHRQNWSYLFRLCYSCASQMIWGWEPIYEIIYANMPINTEMTDFTAVVGKKF..AEGKPLDIPVLSQPYGKRV:160
Ac. S5    RVLQYTWKDWKDHEEMHRQNWSYLFRLCYSCASQMIWGWEPIYEIIYADMPINTEMTDFTAVVGKKF..AEGKPLEIPVISQPYGKRV:160
Su.toko.  MLMQYTFWKNWKDHEEMHKQNWANLFRLCLQCADQMIWGWEPLYEIVYANMPLNTEMTDFTVMVGKKF..AAGEAVSIPPISQPYGKRV:160
Fe.acid.  NVYQYTMWKSIKDHEDMHRENFSSIFRLCSSCLSQVVYGWEPLYEIVDASMPLNTEMADFTTMFGKKF..AAGDPAGVPPISMPYGQRT:158
Aq.aeol.  ELWQYTVWEKWEDHEEMHYQQFDRIFELCVGCFTEVVEGPNEPIYVVRRBANMPPVIDFTDVPKVLGESMMQAMQGKGGIPKVRL.LTQRI:179
Consens.  ..QYT..W...DHE.MH....F.LC..C.....GP.EP.Y...A.MP.......D..T......A...........P......R.: 49

              190      200        210        220      230      240        250      260        270
Ac.ambi.  VAFAEHSVIPGKEKQFEDAIVRTLEMLKK.APGFLGAMVLKEIGVSGIGSMQFGAKGPHQVLENPGSEEPDPNNVMYS.......VPEAK:242
Ac. S5    VAFGEHTVIPGKEKQFEDAILKTLEMFKR.APGFLGAMLLKEIGVSGIGSFQFGSKGPHQLLESPGSFEPDPNNVMYQ.......VPEAK:242
Su.toko.  VAFGEHIVKEGLENQFEEYAIKTLBAFRS.APGFLGNLKTLEIGVSPLGSLQLNAKGPHQILLETANGLDVPEPVTIYE.......APEFR:242
Fe.acid.  IALSEHTVKKDKEKEFESTIVEVMKDFEK.APGFLGYMILKEVGVSAVGSFQLKSKGIHETLLESGGEV.FTQQEGSFK.......PEEAR:239
Aq.aeol.  AVVGIHV.GE.F..GEBKEIEGAVBTLBLLNKYSAGMIGWMILEKIGESPYGTFQIKPPEBWEVVASRGAVPPKTRETLNGEYGKPEFQLEPA:269
Consens.  .H.V..GE.F..........G.GM..L.K.IG.S..G...Q.........P.........E..:63

              280      290        300        310      320      330        340
Ac.ambi.  NTBQQYIVHVEWANTDALMFGMGRVLLYEELRQVHD.EVLDTLVY.GPYIRILNPMMEGTFWREYLNEQ~~:309
Ac. S5    PTBPPQYIVHVEWANLDALMFGMGRVLLSPEYREVHD.EALDTLIY.GPYIRIINPVMEGTFWREYLNE~~:308
Su.toko.  NRBQRYIVHTEWSDTNALMFGLGRVLIYEEVRQIHD.KVLDTLVY.GPYIRVLNPMMEGTYWREYLNEYHL:311
Fe.acid.  PTBPEYKVHMEWASPNDAMFGIGRVLFAHPAREIHD.KVLDTLIR.GPYIRLLNPMMEGTTWREYLNSP~~:306
Aq.aeol.  GHBKEFIVHMEWSRPESAMFGPALTAVNPKIKKVHDEKVMTTLAHIPPYYKVFMPLMEDLILFP~~~~~~~:333
Consens.  .VH.EW....FG......HD....TL....PY....P.ME.......:341
```

Figure 7   Multiple alignment of SOR sequences

#, conserved cysteine residues; *, His-Glu-Xaa-Xaa-His motif known from proteins with mono- and di-iron oxo clusters; †, putative iron-binding residue found in biopterin-dependent tyrosine hydroxylases [35]; cylinders, predicted α-helical regions; open arrows, β-sheet regions for the *Acidianus ambivalens* SOR. *Ac.ambi.*, *Acidianus ambivalens* (GenBank® accession number X56616); *Ac*. S5, *Acidianus* sp. strain S5 (GenBank® accession number AF267286); *Su.toko.*, *Sulfolobus tokodaii* (GenBank® accession number NC_003106; *Fe.acid.*, *Ferroplasma acidarmanus* (Faci1674; GenBank® accession number NZ_AABC02000001); *Aq.aeol.*, *Aquifex aeolicus* (GenBank® accession number NC_000918). Consens., consensus sequence. Immediately upstream of the *Ferroplasma acidarmanus* Faci1674 open reading frame, an in-frame stop codon was found (X, position 49). It was treated as an unknown residue, because of the similarity of the deduced amino acid sequences of the upstream region to the other SOR sequences. It is not known whether this represents a pseudogene or whether *Ferroplasma acidarmanus* produces active SOR under suitable conditions. Black shading indicates identical residues, and grey shading indicates conservative exchanges in at least four of the sequences.

of whether they are known to harbour mononuclear Fe centres or not. In addition, the identification of *sor* genes in other Archaea and in *Aquifex aeolicus*, but not in *Acidithiobacillus ferrooxidans*, *Paracoccus pantotrophus* and other mesophilic bacteria, points to a novel pathway of sulphur oxidation in Archaea and in thermophilic bacteria. It differs both from the Sox pathway found in neutrophilic bacteria [1–3] and the glutathione-dependent sulphur oxygenases of the mesoacidophiles [8–10]. Interestingly, *Aquifex aeolicus* possesses both *sor* and *sox* genes (e.g. [3]), suggesting that elemental sulphur is oxidized by the SOR, whereas the products of the reaction are oxidized by the Sox system. Sox and Sox-related proteins or genes have not been found in *Acidianus ambivalens* so far, which has a membrane-bound thiosulphate:quinone oxidoreductase [14a] and a sulphite acceptor oxido-reductase activity [41].

A multiple alignment of the five SORs showed a His-Xaa₃-His site in the sequence His[86]-Glu-Glu/Asp-Met-His[90]-Glu/Asp-Xaa[38]-Glu/Asp[129] as a putative metal-binding sequence motif (Figure 7), which is similar to the one found in tyrosine hydroxylases containing a mononuclear non-haem iron centre (TyrH; [42,43]). These residues form the structural motif of the 2-His-1-carboxylate facial triad, which anchors the iron in the active site. Secondary-structure prediction identified a putative extensive α-helix including the His-Xaa₃-His box in the SOR sequences (Figure 7). Helix projection suggested that both histidines are facing the same side as in TyrH (results not shown) and that the SORs may adopt a similar structural motif for the iron binding. However, the tentative identification of the possible glutamic acid ligand (Figure 7) is preliminary without additional evidence.
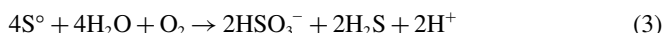
Each SOR has three conserved cysteine residues in common, two of which are arranged as a Cys-Xaa-Xaa-Cys motif (Figure 7). The activity of purified SOR was inhibited by thiol-binding reagents such as *N*-ethylmaleimide and Zn²⁺ ions ([13] and the present study). In consequence, the cysteine residues, or some of

them, must be essential, although it is improbable that they might co-ordinate the metal site as explained above. It is more likely that they play a role in sulphur binding and activation, either as enzyme-bound polysulphide in a similar way as has been described for reduced glutathione [8,9] and for the periplasmatic bacterial sulphur oxygenase [10], or with a disulphide redox chemistry as described for the sulphide:quinone oxidoreductase [44].

The SOR reaction involves complex electron transitions, and it is most likely that more than one redox-active centre is participating in catalysis. The SOR activity is strictly oxygen-dependent. The use of complexed Zn²⁺ ions resulted in a 1:1 stoichiometry of the oxidized and reduced products [13]. The observations can be summed up in two partial reactions consisting formally of an oxygenase reaction (eqn 1) and a sulphur-disproportionation reaction (eqn 2), the latter of which is known to occur non-enzymatically in the presence of hydroxyl ions at pH values of 7.4 and above [13,45]:

$$S° + O_2 + H_2O \rightarrow HSO_3^- + H^+ \tag{1}$$

$$3S° + 3H_2O \rightarrow HSO_3^- + 2H_2S + H^+ \tag{2}$$
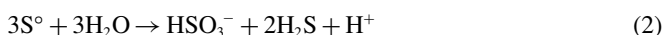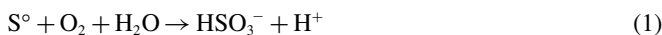
The sum of eqns (1) and (2) gives:

$$4S° + 4H_2O + O_2 \rightarrow 2HSO_3^- + 2H_2S + 2H^+ \tag{3}$$

These interpretations are supported by the rather modest ¹⁸O incorporation observed in the case of the "*Sulfolobus brierleyi*" sulphur oxygenase [15]. It is probable, although it has not yet been demonstrated, that an initial oxygen reduction and activation with sulphur as the electron donor takes place at the iron site. One of the major questions is whether the sulphur reduction or sulphur disproportionation is an indispensable part of the reaction mechanism itself, or whether it is a competing side reaction, i.e. that sulphur can replace oxygen at the iron site. This and the exact

reaction mechanism are unanswered at present and will be the object of future studies.

A shell-like quaternary structure with a central hollow cavity

The well-contrasted dot in the middle of the spherical SOR particles observed in EM images (Figure 4) point to a hollow interior filled with uranyl acetate used for negative staining. Other classes of proteins are known to have this structural feature, most notably the ferritins and the ferritin-like DNA-binding Dps proteins (Figure 4) [46–49]. Electron micrographs of these particles resemble SOR particles, thus strengthening the hypothesis that SOR is a shell-like multimeric protein complex with a hollow core [46,47,49]. The *Desulfovibrio desulfuricans* bacterioferritin is slightly smaller in diameter than the SOR (13.0 nm compared with 15.5 nm, internal hollow core: 8.5 nm). It consists of 24 subunits of a 179-amino-acid protein arranged in dimers and possesses a 432 symmetry (500 kDa molecular mass [48]), whereas Dps proteins are homododecamers with external and internal diameters of 9.0 nm and 4.5 nm respectively, and have a 23 symmetry [50].

It is so far unknown of how many subunits the SOR holoenzyme is actually composed. The molecular mass of the SOR determined by gel-permeation chromatography would point to a 15-mer (550 kDa, 308 amino acid residues [13,14]), whereas the results of the BN PAGE point to a higher molecular mass (732 kDa), equivalent to 20 subunits. A structural model explaining either number of subunits would require the presence of a 5-fold symmetry axis, which was not seen. We calculated the number of atoms fitting into a sphere of the observed size (1950 nm^3), equalling 170 % of the total *Desulfovibrio desulfuricans* bacterioferritin volume (1150 nm^3) not considering its hollow core (322 nm^3). The number of atoms in the holoenzyme would be 178 % of that of the ferritins when assuming 24 subunits. Thus the existence of a 4-fold axis as well as the size of the SOR particles point to a quaternary structure being an icosatetramer with the same overall symmetry as the ferritins, although this conclusion is in contrast with the apparent molecular masses. Preliminary X-ray crystallographic data suggested the presence of an icosatetramer as well (T. Urich and C. Frazão, unpublished work).

CD spectra and secondary-structure-prediction programs agreed well that the SOR should form similar percentages of α-helices and β-sheets of approx. 25 % each. Thus the SOR exhibited a different pattern of secondary-structure elements from the ferritins, which are almost completely made of a four-helix bundle [48], suggesting a different folding pattern.

The tryptophan-fluorescence-monitored experiments showed that the SOR is relatively resistant to unfolding at concentrations of urea up to 4 M, whereas at urea concentrations above 7 M, the fluorescence reached its minimum, indicating a complete denaturation of the enzyme (Figure 3). Monitoring by gel-permeation chromatography showed that a predominant dimer peak was observed up to 5 M urea besides the holoenzyme peak (Figure 2A), whereas the monomer peak appeared at higher urea concentrations. The signal intensities of the holoenzyme and the monomer peaks in the gel-permeation experiment could be superimposed without significant differences to the denaturation curve, which points to a dimer being the building block of the holoenzyme (Figure 2D). This is supported by the results of the BN PAGE showing the dimer band being most prominent in the 2 M urea sample. The fully denatured protein migrated and stained differently in the BN PAGE, suggesting that the denatured enzyme monomers expose more of the hydrophobic residues and aggregate non-specifically, whereas the partially denatured enzyme forms a ladder of bands, presumably showing the holoenzyme in various states of disintegration.

Taking the experiments together, the dimeric state observed in the partially denatured samples in BN gels is properly folded, whereas the complete unfolding of SOR is in good correlation with the appearance of the monomeric state. Furthermore, the data indicate that the assembly of the holoenzyme may proceed via oligomerization of dimers as the building blocks.

Conclusions

We show that a low-potential mononuclear non-haem iron centre is present in the *Acidianus ambivalens* SOR and that this centre is essential for catalytic activity. We also show that the protein is a large oligomer in solution, having a shell-like assembly made of dimers surrounding a central cavity. The data suggest that the iron core and cysteine residues are essential for the enzyme activity, and that iron is co-ordinated by N and O ligands and not by cysteine residues. The most puzzling observation is the sulphur reductase activity of the SOR, although the low reduction potential of the iron core explains the ability to perform this reaction. It cannot yet be decided which of the two possible alternative hypotheses on enzyme activity will prove true: (i) the SOR is a true sulphur-disproportionating enzyme, with the sulphur reductase activity as an inseparable property of the reaction mechanism; or (ii) sulphur competes for the oxygen-binding site and is reduced as a by-product of the enzyme reaction.

REFERENCES

1　Kelly, D. P., Shergill, J. K., Lu, W. P. and Wood, A. P. (1997) Oxidative metabolism of inorganic sulfur compounds by bacteria. Antonie van Leeuwenhoek **71**, 95–107

2　Friedrich, C. G. (1998) Physiology and genetics of sulfur-oxidizing bacteria. Adv. Microb. Physiol. **39**, 235–289

3　Friedrich, C. G., Rother, D., Bardischewsky, F., Quentmeier, A. and Fischer, J. (2001) Oxidation of reduced inorganic sulfur compounds by bacteria: emergence of a common mechanism? Appl. Environ. Microbiol. **67**, 2873–2882

4　Hedderich, R., Klimmek, O., Kröger, A., Dirmeier, R., Keller, M. and Stetter, K. O. (1999) Anaerobic respiration with elemental sulfur and with sulfides. FEMS Microbiol. Rev. **22**, 353–381

5　Kappler, U., Friedrich, C. G., Trüper, H. G. and Dahl, C. (2001) Evidence for two pathways of thiosulfate oxidation in *Starkeya novella* (formerly *Thiobacillus novellus*). Arch. Microbiol. **175**, 102–111

6　Nakamura, K., Nakamura, M., Yoshikawa, H. and Amano, Y. (2001) Purification and properties of thiosulfate dehydrogenase from *Acidithiobacillus thiooxidans* JCM7814. Biosci. Biotechnol. Biochem. **65**, 102–108

7　Boulegue, J. (1978) Solubility of elemental sulfur in water at 298 K. Phosphorus Sulfur **5**, 127–128

8　Suzuki, I. (1965) Oxidation of elemental sulfur by an enzyme system of *Thiobacillus thiooxidans*. Biochim. Biophys. Acta **104**, 359–371

9　Silver, M. and Lundgren, D. G. (1968) Sulfur-oxidizing enzyme of *Ferrobacillus ferrooxidans* (*Thiobacillus ferrooxidans*). Can. J. Biochem. **46**, 457–461

10　Rohwerder, T. and Sand, W. (2003) The sulfane sulfur of persulfides is the actual substrate of the sulfur-oxidizing enzymes from *Acidithiobacillus* and *Acidiphilium* spp. Microbiology **149**, 1699–1710

11　Friedrich, C. G., Quentmeier, A., Bardischewsky, F., Rother, D., Kraft, R., Kostka, S. and Prinz, H. (2000) Novel genes coding for lithotrophic sulfur oxidation of *Paracoccus pantotrophus* GB17. J. Bacteriol. **182**, 4677–4687

12 Rother, D., Henrich, H. J., Quentmeier, A., Bardischewsky, F. and Friedrich, C. G. (2001) Novel genes of the sox gene cluster, mutagenesis of the flavoprotein SoxF, and evidence for a general sulfur-oxidizing system in *Paracoccus pantotrophus* GB17. J. Bacteriol. **183**, 4499–4508

13 Kletzin, A. (1989) Coupled enzymatic production of sulfite, thiosulfate, and hydrogen sulfide from sulfur: purification and properties of a sulfur oxygenase reductase from the facultatively anaerobic archaebacterium *Desulfurolobus ambivalens*. J. Bacteriol. **171**, 1638–1643

14 Kletzin, A. (1992) Molecular characterization of the *sor* gene, which encodes the sulfur oxygenase reductase of the thermoacidophilic archaeon *Desulfurolobus ambivalens*. J. Bacteriol. **174**, 5854–5859

14a Müller, F., Bandeiras, T., Urich, T., Teixeira, M., Gomes, C. M. and Kletzin, A. (2004) Coupling of the pathway of sulfur oxidation to dioxygen reduction: characterization of a novel membrane-bound thiosulfate:quinone oxidoreductase. Mol. Microbiol., in the press

15 Emmel, T., Sand, W., König, W. A. and Bock, E. (1986) Evidence for the existence of a sulphur oxygenase in *Sulfolobus brierleyi*. J. Gen. Microbiol. **132**, 3415–3420

16 He, Z., Li, Y., Zhou, P. and Liu, S. (2000) Cloning and heterologous expression of a sulfur oxygenase/reductase gene from the thermoacidophilic archaeon *Acidianus* sp. S5 in *Escherichia coli*. FEMS Microbiol. Lett. **193**, 217–221

17 Kletzin, A. (1994) Sulfur oxidation and reduction in Archaea: sulfur-oxygenase/-reductase and hydrogenases from the extremely thermophilic and facultatively anaerobic Archaeon *Desulfurolobus ambivalens*. Syst. Appl. Microbiol. **16**, 534–543

18 Sun, C. W., Chen, Z. W., He, Z. G., Zhou, P. J. and Liu, S. J. (2003) Purification and properties of the sulfur oxygenase/reductase from the acidothermophilic archaeon, *Acidianus* strain S5. Extremophiles **7**, 131–134

19 Skerra, A. (1994) Use of the tetracycline promoter for the tightly regulated production of a murine antibody fragment in *Escherichia coli*. Gene **151**, 131–135

20 Nozaki, Y. (1972) The preparation of guanidine hydrochloride. Methods Enzymol. **26**, 43–50

21 Royer, C. A. (1995) Fluorescence spectroscopy. In Protein Stability and Folding: Theory and Practice, vol. 40 (Shirley, B. A., ed.), pp. 65–89, Humana Press Inc., Totowa

22 Shirley, B. A. (1995) Urea and guanidine hydrochloride denaturation curves. In Protein Stability and Folding: Theory and Practice, vol. 40 (Shirley, B. A., ed.), pp. 177–190, Humana Press Inc., Totowa

23 Schägger, H. (1994) Native gel electrophoresis. In A Practical Guide to Membrane Protein Purification (von Jagow, G. and Schägger, H., eds.), pp. 81–106, Academic Press, San Diego

24 Zillig, W., Yeats, S., Holz, I., Böck, A., Rettenberger, M., Gropp, F. and Simon, G. (1986) *Desulfurolobus ambivalens* gen. nov., sp. nov., an autotrophic archaebacterium facultatively oxidizing and reducing sulfur. Syst. Appl. Microbiol. **8**, 197–203

25 Teixeira, M., Batista, R., Campos, A. P., Gomes, C., Mendes, J., Pacheco, I., Anemüller, S. and Hagen, W. R. (1995) A seven-iron ferredoxin from the thermoacidophilic *Desulfurolobus ambivalens*. Eur. J. Biochem. **227**, 322–327

26 Bradford, M. M. (1976) A rapid and sensitive method for the quantitation of microgram quantities of protein utilizing the principle of protein-dye binding. Anal. Biochem. **72**, 248–254

27 Smith, P. K., Krohn, R. I., Hermanson, G. T., Mallia, A. K., Gartner, F. H., Provenzano, M. D., Fujimoto, E. K., Goeke, N. M., Olson, B. J. and Klenk, D. C. (1985) Measurement of protein using bicinchoninic acid. Anal. Biochem. **150**, 76–85

28 Schägger, H. and von Jagow, G. (1987) Tricine-sodium dodecyl sulfate-polyacrylamide gel electrophoresis for the separation of proteins in the range from 1 to 100 kDa. Anal. Biochem. **166**, 368–379

29 Fischer, D. S. and Price, D. C. (1964) Simple serum iron method using new sensitive chromogen tripyridyl-*s*-triazine. Clin. Chem. **10**, 21–25

30 Sreerama, N. and Woody, R. W. (2000) Estimation of protein secondary structure from circular dichroism spectra: comparison of CONTIN, SELCON, and CDSSTR methods with an expanded reference set. Anal. Biochem. **287**, 252–260

31 Schurig, H., Rutkat, K., Rachel, R. and Jaenicke, R. (1995) Octameric enolase from the hyperthermophilic bacterium *Thermotoga maritima*: purification, characterization, and image processing. Protein Sci. **4**, 228–236

32 Schmidt, M., Rutkat, K., Rachel, R., Pfeifer, G., Jaenicke, R., Viitanen, P., Lorimer, G. and Buchner, J. (1994) Symmetric complexes of GroE chaperonins as part of the functional cycle. Science **265**, 656–659

33 Hegerl, R. (1996) The EM program package: a platform for image processing in biological electron microscopy. J. Struct. Biol. **116**, 30–34

34 Saxton, W. O. (1996) Semper: distortion compensation, selective averaging, 3-D reconstruction, and transfer function correction in a highly programmable system. J. Struct. Biol. **116**, 230–236

35 Lange, S. J. and Que, Jr, L. (1998) Oxygen activating non-heme iron enzymes. Curr. Opin. Chem. Biol. **2**, 159–172

36 Nelson, M. (1988) Catecholate complexes of ferric soybean lipoxygenase 1. Biochemistry **27**, 4273–4278

37 Hagedoorn, P. L., Schmidt, P. P., Andersson, K. K., Hagen, W. R., Flatmark, T. and Martinez, A. (2001) The effect of substrate, dihydrobiopterin, and dopamine on the EPR spectroscopic properties and the midpoint potential of the catalytic iron in recombinant human phenylalanine hydroxylase. J. Biol. Chem. **276**, 22850–22856

38 Abreu, I. A., Xavier, A. V., LeGall, J., Cabelli, D. E. and Teixeira, M. (2002) Superoxide scavenging by neelaredoxin: dismutation and reduction activities in anaerobes. J. Biol. Inorg. Chem. **7**, 668–674

39 Vance, C. K. and Miller, A. F. (2001) Novel insights into the basis for *Escherichia coli* superoxide dismutase's metal ion specificity from Mn-substituted FeSOD and its very high E_m. Biochemistry **40**, 13079–13087

40 Thauer, R. K., Jungermann, K. and Decker, K. (1977) Energy conservation in chemotrophic anaerobic bacteria. Bacteriol. Rev. **41**, 100–180

41 Zimmermann, P., Laska, S. and Kletzin, A. (1999) Two modes of sulfite oxidation in the extremely thermophilic and acidophilic archaeon *Acidianus ambivalens*. Arch. Microbiol. **172**, 76–82

42 Costas, M., Mehn, M. P., Jensen, M. P. and Que, Jr, L. (2004) Dioxygen activation at mononuclear nonheme iron active sites: enzymes, models, and intermediates. Chem. Rev. **104**, 939–986

43 Hegg, E. L. and Que, Jr, L. (1997) The 2-His-1-carboxylate facial triad–an emerging structural motif in mononuclear non-heme iron(II) enzymes. Eur. J. Biochem. **250**, 625–629

44 Griesbeck, C., Schutz, M., Schodl, T., Bathe, S., Nausch, L., Mederer, N., Vielreicher, M. and Hauska, G. (2002) Mechanism of sulfide-quinone reductase investigated using site-directed mutagenesis and sulfur analysis. Biochemistry **41**, 11552–11565

45 Roy, A. B. and Trudinger, P. A. (1970) The Biochemistry of Inorganic Compounds of Sulphur, Cambridge University Press, Cambridge

46 Ratnayake, D. B., Wai, S. N., Shi, Y., Amako, K., Nakayama, H. and Nakayama, K. (2000) Ferritin from the obligate anaerobe *Porphyromonas gingivalis*: purification, gene cloning and mutant studies. Microbiology **146**, 1119–1127

47 Kim, B. S., Lee, C. S., Yun, C. Y., Yeo, S. M., Park, W. M. and Kim, H. R. (2001) Characterization and immunological analysis of ferritin from the hemolymph of *Galleria mellonella*. Comp. Biochem. Physiol. A Mol. Integr. Physiol. **129**, 501–509

48 Macedo, S., Romao, C. V., Mitchell, E., Matias, P. M., Liu, M. Y., Xavier, A. V., LeGall, J., Teixeira, M., Lindley, P. and Carrondo, M. A. (2003) The nature of the di-iron site in the bacterioferritin from *Desulfovibrio desulfuricans*. Nat. Struct. Biol. **10**, 285–290

49 Tonello, F., Dundon, W. G., Satin, B., Molinari, M., Tognon, G., Grandi, G., Del Giudice, G., Rappuoli, R. and Montecucco, C. (1999) The *Helicobacter pylori* neutrophil-activating protein is an iron-binding protein with dodecameric structure. Mol. Microbiol. **34**, 238–246

50 Roy, S., Gupta, S., Das, S., Sekar, K., Chatterji, D. and Vijayan, M. (2003) Crystallization and preliminary X-ray diffraction analysis of *Mycobacterium smegmatis* Dps. Acta Crystallogr. D Biol. Crystallogr. **59**, 2254–2256